Food Quality and Safety, 2024, **8**, fyae008
https://doi.org/10.1093/fqsafe/fyae008
Advance access publication 14 February 2024
Article

Article

A visual, rapid, and sensitive detection platform for *Vibrio parahaemolyticus* based on RPA-CRISPR/Cas12a and an immunochromatographic test strip

Jinbin Wang[1,2,4,†], Danhong Xu[3,†], Hua Liu[1], Juan Liu[4], Lemei Zhu[4], Haijuan Zeng[1,2,4,*] and Wenhui Wu[3,*]

[1]The Biotechnology Research Institute, Shanghai Academy of Agricultural Sciences, Key Laboratory of Agricultural Genetics and Breeding, Shanghai, China
[2]Crops Ecological Environment Security Inspection and Supervision Center, Key Laboratory for Safety Assessment of Agricultural Genetically Modified Organisms, Ministry of Agriculture and Rural Affairs, Shanghai, China
[3]School of Food Science and Technology, Shanghai Ocean University, Shanghai, China
[4]School of Public Health, Academician Workstation, Changsha Medical University, Changsha, China

[†]These authors contributed equally to this work.
[*]*Correspondence to*: Haijuan Zeng, The Biotechnology Research Institute, Shanghai Academy of Agricultural Sciences, 2901 Beidi Road, Shanghai 201106, China. E-mail: zenghaijuan12@126.com; Wenhui Wu, School of Food Science and Technology, Shanghai Ocean University, 999 Huchenghuan Road, Shanghai 201499, China. E-mail: whwu@shou.edu.cn

Abstract

Objectives: *Vibrio parahaemolyticus* is the primary species that causes vibriosis. In this study, a point-of-care detection method was developed for *V. parahaemolyticus*.

Materials and Methods: The detection platform targeted the thermolabile haemolysin (*tlh*) gene of *V. parahaemolyticus* based on recombinant polymerase amplification (RPA) and clustered regularly spaced short palindromic repeat (CRISPR/Cas) systems. The platform was combined with an immunochromatographic test strip (ICS) that enables low-cost, simple, visual detection of *V. parahaemolyticus*.

Results: The detection limit was 2.5×10^2 fg/μL for plasmids and 1.4×10^2 CFU/mL for *V. parahaemolyticus*. In addition, *V. parahaemolyticus* in salmon sashimi could be detected at a concentration of 154 CFU/g without enrichment, and the entire detection time was around 30 min. After enrichment for 6 h, 2 CFU/g *V. parahaemolyticus* could be detected.

Conclusions: Consequently, the proposed RPA-CRISPR/Cas12a-ICS platform could detect *V. parahaemolyticus* in seafood intuitively, quickly, and sensitively, leading to high practical application value.

Keywords: CRISPR/Cas12a; immunochromatographic test strip; *tlh*; *Vibrio parahaemolyticus*.

Introduction

Rising ocean temperatures and ocean acidification resulting from climate change have led to increased *Vibrio* abundances in oceans that have attracted widespread attention from global researchers (Zha *et al*., 2023). The overall incidence of vibriosis in 2021 increased by 45.5% compared with the annual incidence in 2016–2018 based on the most recent FoodNet (USA) annual report (Boraschi-Diaz *et al*., 2018). Furthermore, *V. parahaemolyticus* accounted for 59.5% of the total number of laboratory-confirmed vibriosis cases in 2015, and it is the only foodborne bacterial pathogen in the USA that exhibits increased incidence in recent years (Collins *et al*., 2022; Neil *et al*., 2023).

V. parahaemolyticus is a Gram-negative halophilic, rod-shaped bacterium found in marine, coastal, and estuarine environments, in addition to being the primary pathogen responsible for acute hepatopancreatic necrosis that is also referred to as early death syndrome (Rosilan *et al*., 2023). The surface and intestines of seafood are the main sites for the attachment of *V. parahaemolyticus*, and the bacteria on the surface of seafood can contaminate ready-to-eat sashimi during cutting or handling (Bai *et al*., 2023; Yu and Rhee, 2023). Raw consumption of fish and shellfish is the main cause of foodborne outbreaks related to *V. parahaemolyticus*. There are essentially no mechanisms that could prevent *V. parahaemolyticus* from entering the food supply chain, unlike many other foodborne pathogens (Hyun, 2009). Therefore, point-of-care testing (POCT) is particularly important for managing *V. parahaemolyticus* contamination.

Most routine detection methods for *V. parahaemolyticus* rely on traditional techniques for microbial isolation, culture, and biochemical identification (Chamchoy *et al*., 2022). However, these traditional detection methods require large workloads and long detection times that do not fully meet

Received 27 September 2023; Revised 21 December 2023; Editorial decision 30 January 2024

the requirements and challenges of food safety supervision and food enterprises for accurate, rapid, and convenient detection of *V. parahaemolyticus*. Varying biosensors including electrochemical-based (Nguyen and Gu, 2023), surface plasmon resonance (Zhou *et al*., 2023), and surface-enhanced Raman scattering-based (Wei *et al*., 2022) sensors have recently been used to detect bacteria and exhibit significant advantages compared with traditional culture-based methods. However, these methods require highly trained operational skills in addition to expensive and cumbersome equipment that are not conducive to POCT.

Molecular detection methods such as multiple polymerase chain reaction (PCR) (Yin *et al*., 2023) and real-time PCR (Kilic and Basustaoglu, 2011) have also been used for bacterial identification and quantification, but require expensive thermal cycling equipment and protocols that are time-consuming and labor-intensive. In contrast, isothermal DNA amplification mediated by recombinant enzyme polymerase amplification (RPA) has recently been shown to harbor great potential application in POCT molecular diagnosis due to the rapid reaction time, simple operation, and constant temperature associated with amplification (Lin *et al*., 2023; Liu *et al*., 2023).

Clustered regularly interspaced short palindromic repeat (CRISPR) systems comprise an adaptive immunity system in Bacteria and Archaea (Hille *et al*., 2018). CRISPR systems can be divided into two broad categories based on differences in structure and function, in addition to the genetic content (Makarova *et al*., 2015). Cas12a is a class 2 CRISPR-Cas system. The second major type of system comprises single multidomain Cas proteins that are more homogeneous and exhibit simpler organization than the first type of system (Xiao *et al*., 2023). The Cas12a enzyme recognizes adjacent motifs in the T-nucleotide-rich primary spacer region, catalyzes the maturation of self-directed CRISPR-RNA (crRNA), and generates distal dsDNA breaks of protospacer adjacent motif with interlaced 5′ and 3′ ends (Chen *et al*., 2018; Fernandez *et al*., 2018). In addition, transmembrane activity and target DNA binding can induce non-target DNA breakage of Cas12a that is referred to as *trans*-cleavage activity (Li *et al*., 2018). The CRISPR/Cas12a system and nucleic acid amplification have been combined to achieve highly sensitive detection of human papillomavirus genes (Chaijarasphong *et al*., 2019; Su *et al*., 2022).

In this study, a specific, visual, and rapid detection strategy for *V. parahaemolyticus* was developed. This strategy was the first application to combine RPA amplification technology with CRISPR/Cas12a to detect the specific gene thermolabile haemolysin (*tlh*) of *V. parahaemolyticus*. RPA was combined with the CRISPR/Cas12a system to eliminate false positives from isothermal amplification. The combination of RPA-CRISPR/Cas12a with an immunochromatographic test strip (ICS) consequently leads to rapid visual detection of *V. parahaemolyticus*.

Materials and Methods

Materials

All primers, crRNAs, and ssDNAs were synthesized by Sangon (Shanghai, China). RPA assay kits, LbCpf1 nuclease, a TIANamp bacterial DNA Kit (model DP302), a plasmid Mini-Prep kit, and RNase Inhibitor were acquired from Tiangen (Beijing, China), TwistDx (Cambridge, MA, USA), BBI (Shanghai, China), Sangon, and Tolobio (Shanghai, China), respectively. Brain heart infusion broth (BHI), biotin ligand, streptavidin, goat anti-rabbit antibody, bovine serum albumin, anti-FITC antibody (conjugated gold-nanoparticles (AuNPs), 15 nm), and anti-FITC antibody were purchased from Beijing Land Bridge (Beijing, China), Merck Chemicals (Shanghai, China), Beijing Biosynthesis Biotechnology (Beijing, China), and Solarbio (Beijing, China), respectively. Nitrocellulose (NC) membranes (CN95 and CN140), cellulose fiber absorbent pads, fiberglass mats (sample pads and conjugate pads), and PVC backing plates were purchased from Merck Chemicals (Shanghai, China).

Thirteen bacterial strains including two types of *V. parahaemolyticus* and 11 other common foodborne pathogens were selected for analysis (Table S1). Salmon was purchased from the local agricultural products wholesale market (Long Shang, Shanghai, China). All solvents and other chemicals were of analytical grade.

Genomic DNA extraction

Strains were cultured for 12 h under cultivation conditions as shown in Supporting Information (Table S1). Then, 1 mL of a pure culture suspension was collected for genomic DNA extraction using a bacterial DNA extraction mini kit, and 2 μL of the extraction was used as an amplification template for specificity detection.

To evaluate detection sensitivity, the boiling method was used to extract genomic DNA. The plate counting method was first used to determine the number of viable bacteria in the samples (1.4×10^6–1.4 CFU/mL). Then, 1 mL of the culture was centrifuged at 12 000×*g* for 2 min, followed by discarding 800 μL supernatant. The remaining 200 μL of the solution was evenly mixed and subjected to cracking at 100 °C for 10 min, followed by incubation in an ice bath for 5 min and centrifugation at 12 000×*g* for 2 min. Then, 5 μL of the crude extract was used as an amplification template. All extracted genomic DNA was stored at –20 °C.

Primer, crRNA, and ssDNA design

The whole genome sequences of 13 *V. parahaemolyticus* were retrieved from the National Center for Biotechnology Information (USA) database, and the *tlh* gene fragment (GenBank No. M36437) specific to *V. parahaemolyticus* was evaluated to explore detection targets (Table S2). The RPA primers used in this study were designed using Primer Premier 5.0 (Premier Biosoft, Vancouver, Canada), and crRNAs were designed using the CRISPOR online platform (http://crispor.tefor.net/). Detailed design information is shown in Table S2.

Plasmid construction

To construct a standard reference plasmid for absolute sensitivity experiments, the RPA amplification product confirmed by sequencing was cloned into the pUC57 vector. After purification using the plasmid miniprep kit, the concentration of the recombinant plasmid was determined using a NanoDrop 2000c instrument (Thermo Scientific, Waltham, MA, USA) to calculate the molecular copy number of the recombinant plasmid. The plasmids were then diluted to 2.5×10^5, 2.5×10^2, 100, 50, 25, 10, and 2.5 copies/μL with TE buffer and used to evaluate assay sensitivity by observing T- and C-lines of the test strips.

Construction and analysis of ICS

ICS composition is shown in Figure S1. Two micrograms of AuNP-labelled anti-FITC antibody was coated on the conjugate pad and used for coloration. To construct control (C-line) and test (T-line) lines, streptavidin (2 mg/mL) and goat anti-rabbit IgG antibody (1 mg/mL) were distributed onto the NC membrane (volume of 1 μL/cm) using the BioDot-XYZ3060 dispensing system (Bio-Dot, Irvine, CA, USA). The absorbent pad, sample pad, conjugate pad, and NC membrane were sequentially assembled on the plastic backing board with an overlap of 1.5–2 mm. The ICS was then sectioned into 3-mm wide strips using a CM4000 cutter (Bio-Dot, Irvine, CA, USA). Finally, the prepared ICS was sealed in a plastic bag with a desiccant at room temperature.

For ICS analysis, 5 μL of the enzymatic cleavage products was loaded onto the sample pad, and the ICS with cleavage products was placed in a tube containing 70 μL phosphate buffer solution. After 5 min, visual results were obtained.

RPA detection system

The RPA process was performed following the instructions of RPA assay kits. First, 29.5 μL of Primer Free Rehydration buffer was thoroughly mixed with 11.2 μL or 8.2 μL of ddH_2O and then added to the dry enzyme powder to completely dissolve the powder. Then, 2.4 μL of primers and 2 μL or 5 μL of plasmid molecule or bacterial genome DNA were added to the sequence and fully mixed. Finally, 2.5 μL of MgOAc was added to initiate the reaction, followed by incubation at 40 °C for 10 min.

CRISPR/Cas12a-ICS and fluorescence detection system

The CRISPR/Cas12a assay contained 100 nmol/L LbCpf1 nuclease, 10 U of RNase inhibitor, 250 nmol/L ssDNA reporter, 200 nmol/L crRNA, 2 μL NE buffer, and 2 μL of dsDNA target within a total 20 μL reaction volume. The DNA template was the RPA product, and the ssDNA was a non-targeting probe. The ssDNA reporter of ICS was biotin- and FITC-double-labelled (5′-biotin-(TTATT)3-FITC-3′), and a flu-ssDNA reporter (5′-HEX-10T-BHQ1-3′) was designed for fluorescence detection. Real-time fluorescence detection was performed in a 384-well plate and incubated at 40 °C in a multipurpose microplate reader (Tecan, Mannedorf, Switzerland), with fluorescence measurements taken at 1 min intervals (λEx: 530 nm, λEm: 560 nm). The RPA amplified products of DNase/RNase-free distilled water or bacteria-free samples were used as negative controls.

Specificity and sensitivity of the RPA-CRISPR/Cas12a-ICS platform

The specificity and sensitivity of the proposed method were evaluated to ensure reliability. Two *V. parahaemolyticus*, two *Vibrio* spp. (*V. vulnificus* and *V. algolyticus*), and nine non-*V. parahaemolyticus* spp. strains (Table S1) were used to validate the specificity of the RPA-CRISPR/Cas12a platform. The sensitivity of the RPA-CRISPR/Cas12a-ICS platform was evaluated at various bacterial concentrations ranging from 1.4×10^6 to 1.4 CFU/mL. The absolute sensitivity of RPA-CRISPR/Cas12a-ICS was also evaluated at various concentrations ranging from 2.5×10^5, 2.5×10^4, 2.5×10^3, 2.5×10^2, 100, 50, 25, and 2.5 copies/μL. DNase/RNase-free distilled water was used as a non-template control.

Sample validation

To detect artificially contaminated samples, the purchased fresh salmon sashimi was placed on a super clean platform for UV sterilization over 0.5 h. Salmon was infected with *V. parahaemolyticus* at final concentrations of 2, 154, 3.6×10^4, and 1.2×10^6 CFU/g, respectively. The strains contaminate food from the surface, so disposable Q-tips were used to wipe the salmon and collect *V. parahaemolyticus*. Then, the disposable Q-tip was placed in a 1.5-mL centrifuge tube containing 200 μL deionized water. DNA was extracted using the heat-splitting method. Finally, RPA-CRISPR/Cas12a-ICS platform was used for detection, and three replicates were used for each test.

To detect low-concentration contaminated samples, spiked salmon (2 CFU/g) was incubated in 225 mL of BHI medium at 37 °C. At 1 h intervals, 2 mL of culture was collected for genomic DNA extraction. Then, RPA-CRISPR/Cas12a-ICS platform was used for detection.

In order to evaluate the practical application of the RPA-CRISPR/Cas12a-ICS platform, 20 food samples were purchased and collected for testing in this study (detailed information is shown in Table S3). Samples were tested using RPA-CRISPR/Cas12a-ICS platform and the national standard method of China (GB 4789.10-2016; NHC and SAMR, 2016), respectively.

Statistical analyses

The test strip results were directly visually determined without instrumentation. Intensities of fluorescence data for the RPA-CRISPR/Cas12a method were collected and analyzed using the GraphPad Prism 7.0 program (La Jolla, CA, USA). Data analysis and graphing were performed in Origin 2021 (OriginLab, Northampton, MA, USA) with the SPSS software package (version 23.0; IBM Crop., Chicago, IL, USA). The means±standard deviation were observed for at least three independent experiments for all measurements.

Results

Principle of the RPA-CRISPR/Cas12a-ICS platform

To detect *V. parahaemolyticus* in foods quickly, sensitively, and specifically, an RPA-CRISPR/Cas12a detection platform was successfully established in combination with ICS. Four steps used to detect *V. parahaemolyticus* (Figure 1) include (i) genomic DNA extraction of *V. parahaemolyticus* from the sample, (ii) genomic DNA amplification of *V. parahaemolyticus* using RPA, (iii) identification and cleavage of the target gene *tlh* using the CRISPR/Cas12a system, and finally (iv) signal detection from ICS.

When the amplified target sequences hybridized with complementary crRNA, *trans*-cleavage activity was triggered by binary complexes, resulting in the cleavage of ssDNA reporters in the reaction solution. When *trans*-cutting was activated in the RPA-CRISPR/Cas12a-ICS platform, ICS ssDNA reporters were cleaved to produce two ssDNA fragments labeled with biotin and FITC. The ssDNA fragments labelled by FITC then bound AuNP-labelled anti-FITC antibodies to form new complexes on the binding pad. Under capillary action, the complex moves to the T line and binds to the goat anti-mouse IgG antibody, turning the T line red.

Primer, crRNA, and ssDNA screening

To improve the sensitivity of the RPA-CRISPR/Cas12a platform, two RPA primers were designed for amplification.

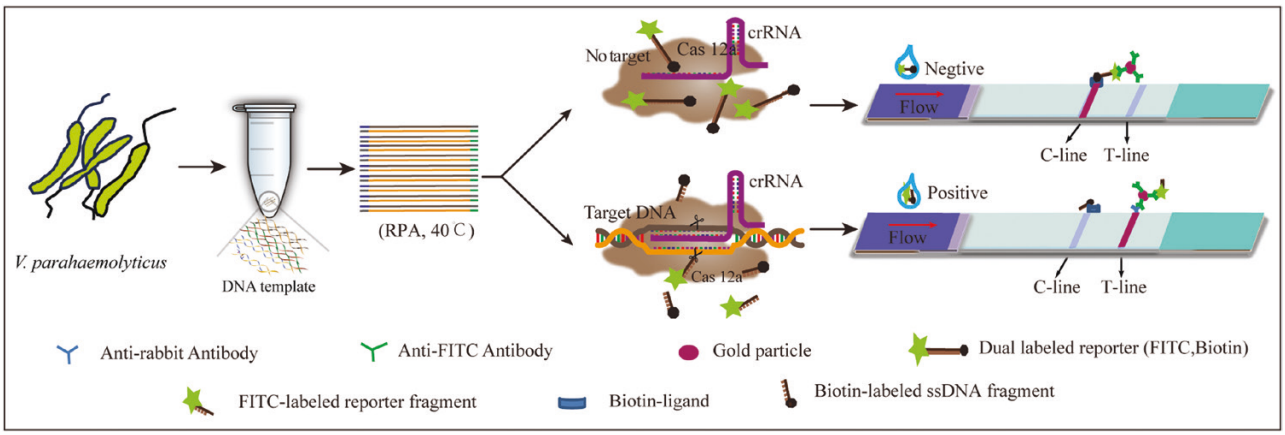

Figure 1. Schematic showing the use of a CRISPR/Cas12a system combined with isothermal amplification and ICS for rapid and visual nucleic acid detection.

The RPA-1 primer exhibited brighter bands than RPA-2 (Figure 2A), and no primer dimerization was identified in the negative control. Two crRNAs were designed to improve cleavage efficiency for the RPA-CRISPR/Cas12a platform. The highest fluorescence intensity of crRNA1 (Figure 2B) was found by comparison with that of the negative control. Evaluation of the RPA-CRISPR/Cas12a dynamics revealed that crRNA1 exhibited a stronger fluorescence response (Figure 2C) compared with crRNA-2 (Figure 2D), consistent with the relative fluorescence intensity results.

To improve the sensitivity of the test strip, three ssDNAs were designed and evaluated for *V. parahaemolyticus* detection at concentrations of 10^4 CFU/mL and 10^3 CFU/mL. T lines for the three ssDNA negative controls were not observed, while ssDNA-3 was the most obvious and exhibited the highest sensitivity at 10^3 CFU/mL (Figure 2E).

Optimization of the RPA-CRISPR/Cas12a-ICS assay

The reaction conditions of RPA, the CRISPR/Cas12a system, and the concentration of ssDNA were optimized. The optimized results of RPA amplification conditions are shown in Figure 3. When the RPA amplification temperature was 40 °C, the relative fluorescence intensity was highest (Figure 3A3), which was consistent with the gel electrophoresis results (Figure 3A1). When the RPA reaction lasted more than 10 min, and the time had little effect on the signal enhancement (Figure 3A4). Therefore, 10 min was chosen as the optimal reaction time.

CRISPR/Cas12a-based detection is based on an enzymatic reaction, with the detection capacity closely related to reaction temperature, concentration of enzymes, and other parameters. The optimal temperature was observed at 40 °C (Figure 3C1), leading to a stronger fluorescence response compared with commonly used temperatures (37 °C) and higher temperatures (43 °C). The amount of Cas12a enzyme significantly affects CRISPR/Cas12a reactions and enzyme cleavage reactions. The fluorescence response of Cas12a at 50 nmol/L was the lowest (Figure 3C2), while concentrations of Cas12a above 100 nmol/L had almost no effect on signals enhancement. To ensure cost efficiency through reagent costs, a 100-nmol/L Cas12a concentration per reaction was selected as the optimal concentration. The ratio of Cas12a to crRNA was also optimized, with 1:2 identified as optimal (Figure 3C3).

Finally, the probe concentration was optimized. When target DNA was not added, the T line was not observed, while the C line was clearly visible. When the probe concentration was between 1250 nmol/L and 250 nmol/L, as the probe concentration decreased, the T-line signal significantly deepened (Figure 3B1), and the C-line signal gradually weakened (Figure 3B2). When the probe concentration was lower than 250 nm, the T-line signal gradually weakened, and the C-line signal significantly enhanced. When the target DNA was present and the probe concentration was 250 nmol/L, the T line was the clearest and the C-line signal was the weakest; most importantly, the background signal was the weakest, showing a normal negative band. Consequently, 250 nmol/L was identified as the most suitable probe concentration. Overall, a reaction temperature of 40 °C, 100 nmol/L Cas12a, 250 nmol/L of ssDNA reporters, and a 1:2 ratio of Cas12a to crRNA were identified to achieve optimal reaction conditions.

Specificity and sensitivity of the RPA-CRISPR/Cas12a platform

To ensure the specificity of the RPA-CRISPR/Cas12a-ICS platform, 13 strains, including two *Vibrio* spp. (*V. vulnificus* and *V. algolyticus*) and nine non-*Vibrio* spp. strains, were evaluated (Table S1). Only the target strain exhibited a strong signal on the T line, while strains without the *tlh* gene did not produce a signal on the T line (Figure 4B1). Similarly, only the target strain produced a strong fluorescent signal (Figure 4A1, $p<0.05$), which was consistent with the electrophoresis results (Figure 4C1). Thus, the RPA-CRISPR/Cas12a-ICS platform exhibited high specificity.

To evaluate the sensitivity of the platform, plasmids at concentrations ranging from 2.5×10^5 to 2.5 copies/μL and *V. parahaemolyticus* at concentrations ranging from 1.4×10^6 to 1.4 CFU/mL were prepared. The limit of detection (LOD) of the RPA-CRISPR/Cas12a-ICS platform for plasmid DNA (Figure 4B2) was consistent with the relative fluorescence intensity (Figure 4C2) and electrophoresis results (Figure 4A2), all of which yielded an LOD of 2.5×10^2 copies/μL. In addition, relative fluorescence could detect *V. parahaemolyticus* at 1.4 CFU/mL (Figure 4C3). The LOD of the RPA-CRISPR/Cas12a-ICS platform was 1.4×10^2 CFU/mL (Figure 4B3),

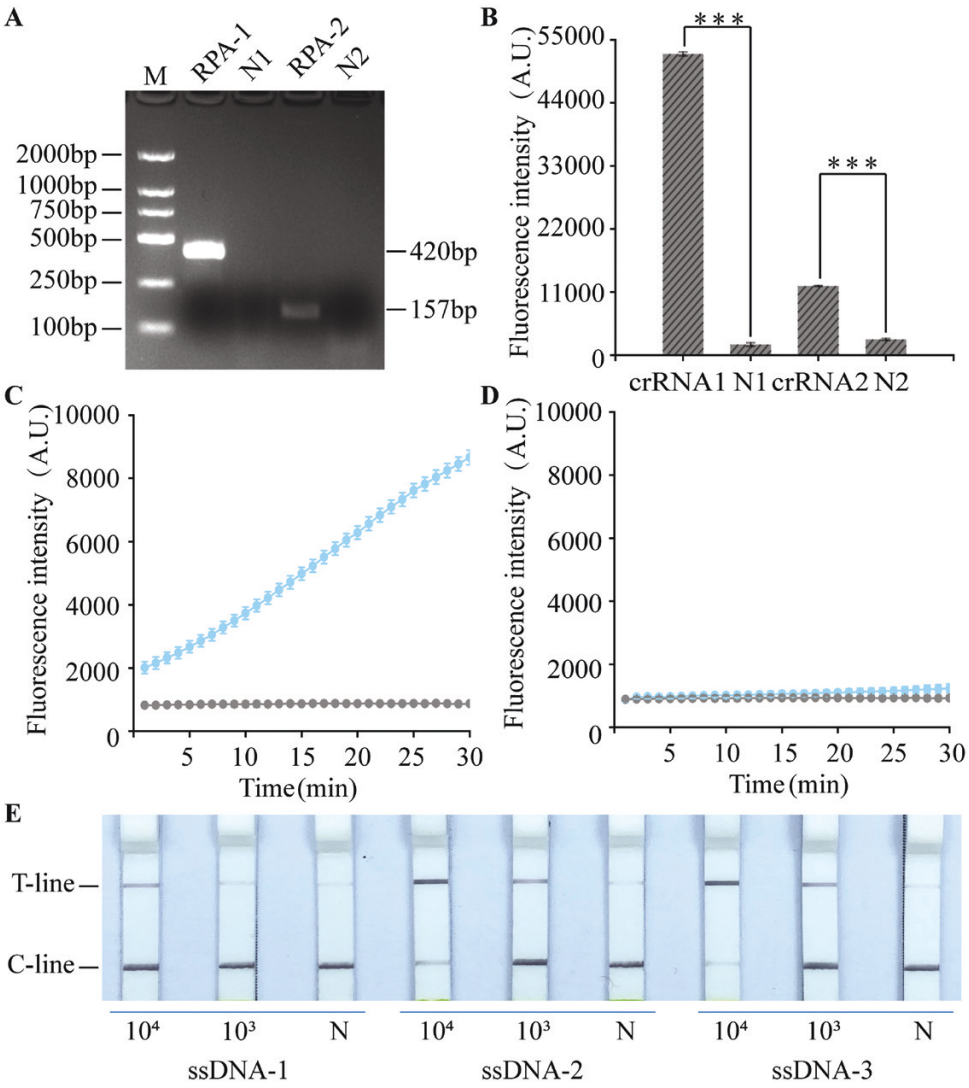

Figure 2. Screening of RPA primers, crRNA, and ssDNA used in the RPA-CRISPR/Cas12a-ICS assay. (A) Visualization of amplification products from different RPA primers by agarose gel electrophoresis. (B) Relative fluorescence intensity of RPA-CRISPR/Cas12a with different crRNA involvement. (C, D) RPA-CRISPR/Cas12a system dynamics with crRNA-1 or crRNA-2 based on microplate reader measurements. (E) RPA-CRISPR/Cas12a-ICS detection of different ssDNAs in the genomic DNA from different concentrations of *V. parahaemolyticus* (10^4, 10^3, 0 CFU/mL; $p<0.05$, with three biological replicates). M, DL2000 marker; N, negative control without template added.

which was 10 times higher than that of the gel electrophoresis analysis (Figure 4A3).

The applicability for food contaminated artificially with *V. parahaemolyticus*

To verify the feasibility of the RPA-CRISPR/Cas12a-ICS method for detecting *V. parahaemolyticus* in food substrates, salmon samples were infected with *V. parahaemolyticus* at 2, 154, 3.6×10^4, and 1.2×10^6 CFU/g, followed by DNA extraction and detection. The official national food safety standard of China, GB 29921-2021 (NHC and SAMR, 2021), sets the LOD for *V. parahaemolyticus* at 10^3 CFU/g. The RPA-CRISPR/Cas12a-ICS platform could detect spiked samples at a culture concentration of 154 CFU/g without enrichment (Figure 5A), which was 6.5 times higher than the LOD proposed in the national standard of China. In subsequent experiments, 2 CFU/g contaminated samples could be detected using the methods proposed in this study after enrichment for 6 h.

Evaluation of the practical value of the RPA-CRISPR/Cas12a platform

In addition to the above analysis, 20 food samples were collected from local markets to evaluate the practical application of the RPA-CRISPR/Cas12a-ICS platform. The RPA-CRISPR/Cas12a-ICS platform identified positive samples for birth oysters and clams (Figure 6A), consistent with the results from the national standard testing method of China (GB 4789.10-2016; Figure 6B). Thus, the platform exhibited satisfactory accuracy for detection in real-world samples.

Discussion

Vibrio parahaemolyticus has caused significant increases in the incidence of infections to a greater extent relative to other foodborne pathogens over the past two decades. These infections primarily occur due to the consumption of raw fish and seafood such as shellfish (Hyun, 2009;

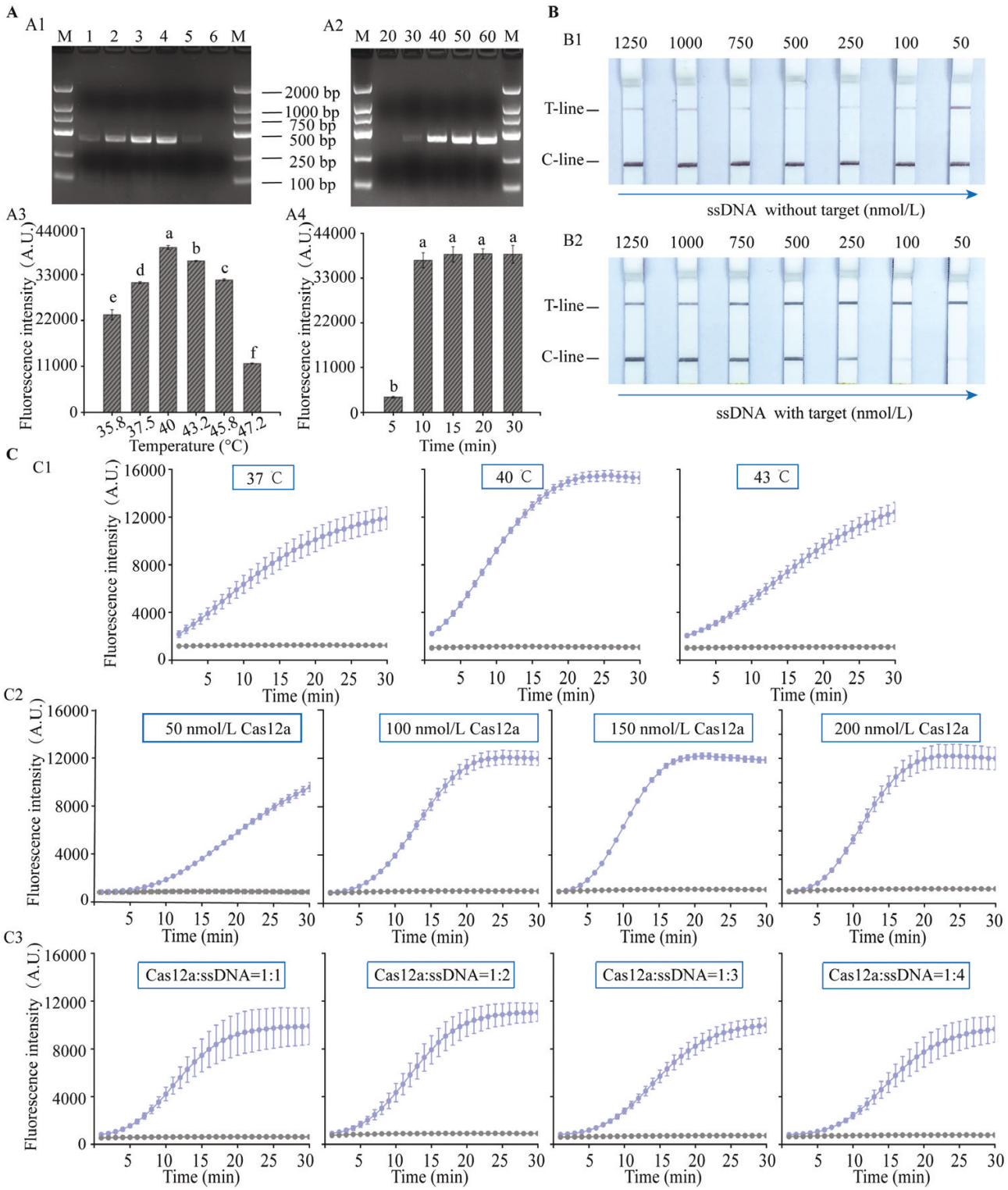

Figure 3. Optimization of the RPA-CRISPR/Cas12a assay and ssDNA concentration. (A1, A2) Visual detection of RPA products by gel electrophoresis. (A3, A4) Relative fluorescence intensity of RPA-CRISPR/Cas12a. (B1, B2) RPA-CRISPR/Cas12a-ICS determination of *V. parahaemolyticus* with and without target DNA at different ssDNA concentrations. (C1, C2, C3) RPA-CRISPR/Cas12a dynamics observed using a microplate reader at different temperatures, concentrations of Cas12a, and concentrations of Cas12a and crRNA, respectively. M, DL2000 marker; N, no template was added as a negative control.

Ashrafudoulla *et al.*, 2021). Some studies have reported systems to detect *V. parahaemolyticus*, including through the combination of electrochemistry with duplex PCR (Campàs *et al.*, 2023) and PMA-mPCR (Hu *et al.*, 2023) detection, in addition to detection with dual-mode colorimetric electrochemical biosensors (Wang *et al.*, 2023). However, these methods require expensive and bulky instruments and cannot achieve POCT for detecting *V. parahaemolyticus*. In

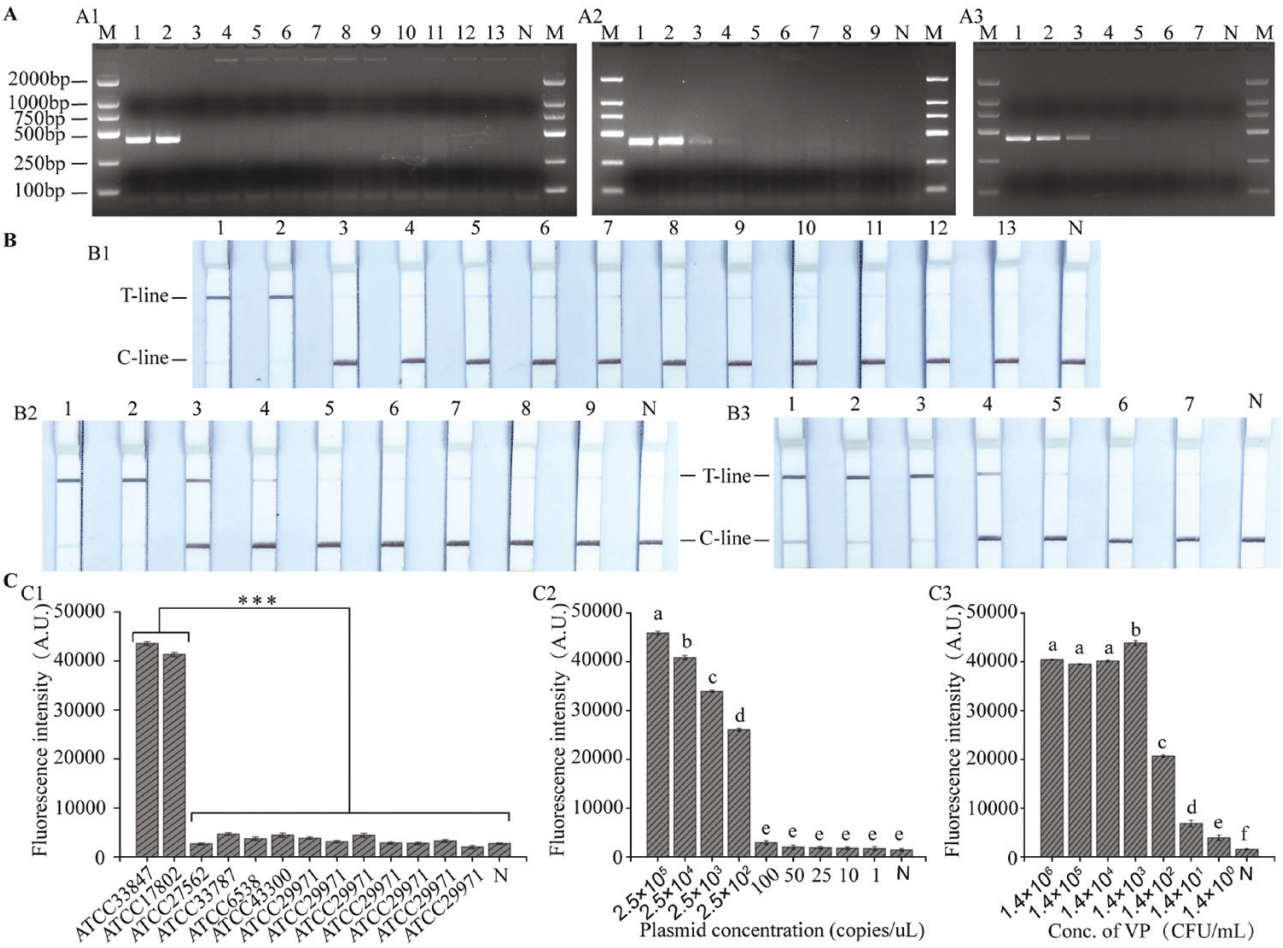

Figure 4. Detection specificity and sensitivity of the RPA-CRISPR/Cas12a platform. (A1, A2, A3) Visual detection of RPA-specificity, plasmids, and *V. parahaemolyticus* strain pure culture products by gel electrophoresis, respectively. (B1, B2, B3) Sensitivity of the RPA-CRISPR/Cas12a-ICS platform for specific detection of *V. parahaemolyticus*, plasmids, and *V. parahaemolyticus* strain pure cultures, respectively. (C1, C2, C3) Sensitivity evaluation based on relative fluorescence intensity evaluation of specificity, plasmids, and pure cultures of *V. parahaemolyticus*, respectively, using the RPA-CRISPR/Cas12a platform to detect *V. parahaemolyticus*. Each measurement comprised three biological replicates, $p<0.05$. Lanes 1–13 in A1 and B1 correspond to the sample names in C1, while lanes 1–9 in A2 and B2 correspond to those in C2 and lanes 1–7 in A3 and B3 correspond to the sample names in C3. N, no template was added as the negative control.

this study, an RPA-CRISPR/Cas12a-ICS platform was successfully constructed and applied for the POCT detection of *V. parahaemolyticus*.

A high-sensitivity RPA-CRISPR/Cas12a-ICS platform is dependent on (1) the efficiency of genome extraction, (2) the concentration and length of the biotin-ssDNA reporter probes, and (3) the CRISPR/Cas12a reaction system. In nucleic acid-based detection methods, the extraction efficiency of nucleic acids greatly affects the LOD, and thus the sensitivity and practical application values of the systems. In this study, the nucleic acid extraction method of GB 29921-2021 (NHC and SAMR, 2021) was first improved, resulting in a shortening of the centrifugation time to 2 min and increasing heating temperature to 100 °C. The entire process does not require the addition of any reagents, thereby lessening the need for extraction reagents and simplifying operation steps.

The length, sequence, and concentration of the ssDNA probes significantly affected the RPA-CRISPR/Cas12a-ICS strip analysis of Cas12a *trans*-cleavage products. Specifically, the 15-bp ssDNA probes provided more spatial locations compared with the 5-bp and 8-bp ssDNA probes, thereby improving the capture of biotin-ligand. Concomitantly, the ssDNA probe concentration deviated from the appropriate range, resulting in T-line banding under negative conditions and an increased probability of false positive results. If the probe quantity is insufficient, excess AuNP complexes will flow to the T line with the buffer, resulting in false positives. However, if the number of ssDNA probes is too high, a high-dose crochet effect occurs and the T line of the test strip is observed. The ssDNA probe was consequently optimized, with 250 nM of the ssDNA probe proving suitable for strip analysis.

This CRISPR/Cas12a reaction system was also optimized in this study, the optimal reaction conditions were when the concentration of Cas12a was 100 nmol/L and the ratio of Cas12a to crRNA was 1:2, and the results were consistent with the study of Chen *et al.* (2022). The optimal reaction temperatures nevertheless differed between studies, which may be due to the use of different types of Cas12a enzymes.

To fully assess our strategy, some relevant assays on *V. parahaemolyticus* are listed in Table S4. This study was the first to combine RPA-CRISPR/Cas12a with ICS to detect *V. parahaemolyticus* in food. It is more portable than

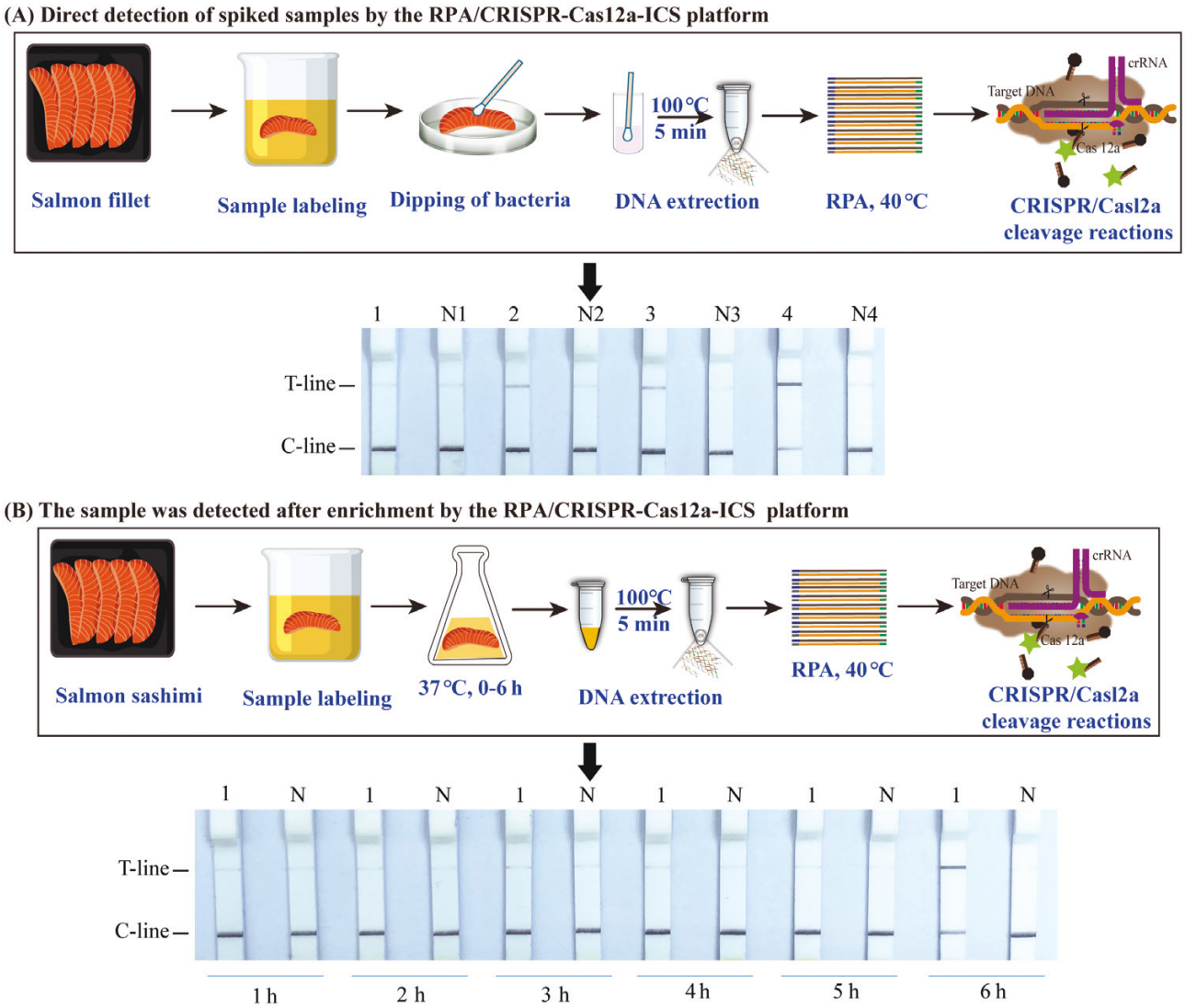

Figure 5. The use of the RPA-CRISPR/Cas12a-ICS platform to detect spiked samples. (A) Use of the RPA-CRISPR/Cas12a-ICS platform to detect *V. parahaemolyticus* spiked into salmon samples at different concentrations. (B) Use of the RPA-CRISPR/Cas12a-ICS platform to detect *V. parahaemolyticus*-spiked samples at different cultivation times. Numbers 1–4 represent salmon samples with different concentrations of 2, 154, 3.6×10^4, and 1.2×10^6 CFU/g; N, no *V. parahaemolyticus* was added as the negative control.

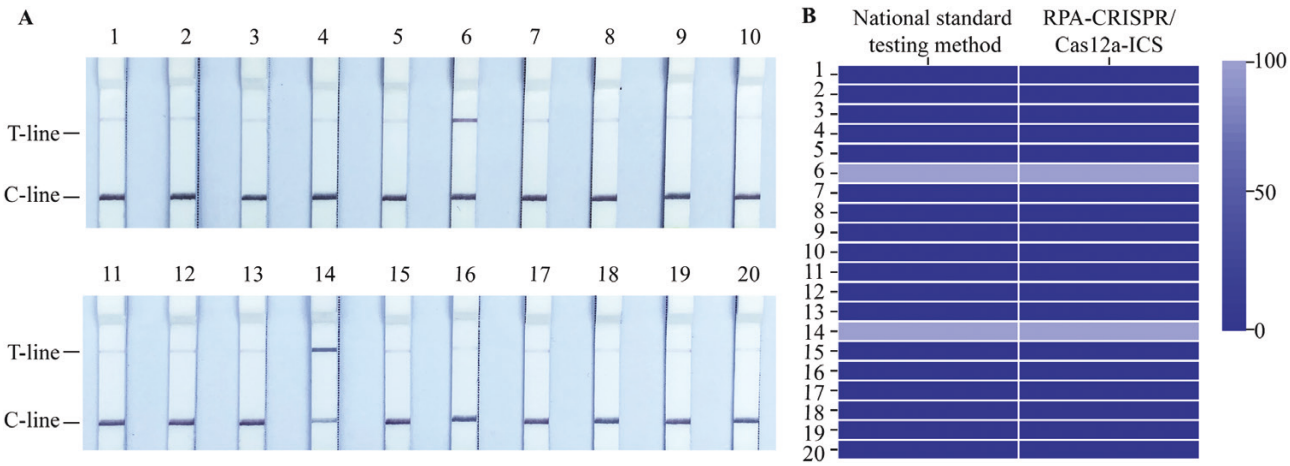

Figure 6. Evaluation of the RPA-CRISPR/Cas12a-ICS platform for natural sample detection. (A) Use of the RPA-CRISPR/Cas12a-ICS platform for detecting *V. parahaemolyticus* in 20 samples collected from a market. (B) The performance of the RPA-CRISPR/Cas12a-ICS platform for *V. parahaemolyticus* detection in food samples compared with standard culture detection.

method No. 1 and does not require additional excitation light of specific wavelengths. Method No. 2 had a detection sensitivity of 100 CFU/mL, which was similar to this study, but the detection time was 120 min longer than that in this paper. Although the Nos. 3 and 4 detection methods improved the detection sensitivity, the detection time costs were higher than those in this paper. Method No. 5 achieved high-throughput detection, but the detection sensitivity (10^4 CFU/mL) was 100 times lower than that of the proposed method. In conclusion, this study has advantages over existing studies in terms of detection portability, sensitivity, and detection duration.

In addition, change in crRNA sequences could lead to the identification of other targets, so that the optimized ssDNA concentration could also be used for any other detection targets. Thus, the RPA-CRISPR/Cas12a-ICS platform could be used to detect foodborne pathogens closely associated with humans, as well as adulterated foods and even viruses.

Conclusions

In this study, a convenient, visual, sensitive, and specific POCT detection platform was developed that integrates RPA, CRISPR/Cas12a detection, and ICS to detect the *tlh* gene specific to *V. parahaemolyticus*. The platform features several advantages. First, samples are pretreated by pyrolysis, which is simpler and faster than most other sample treatment methods. Furthermore, the use of RPA realizes the exponential amplification of nucleic acids, while also avoiding the need for a complex thermal cycling apparatus. In addition, signal transduction is achieved through ICS, which is a visual and portable detection method. The detection of *V. parahaemolyticus* with the platform can be accomplished in approximately 30 min, with an LOD of 250 copies/μL for plasmid samples and 140 CFU/mL for bacteria. The platform was validated in artificially contaminated food samples and with various clinical isolates. Moreover, the platform met the requirements for POCT detection of *V. parahaemolyticus* and may be of great significance for food safety supervision and clinical diagnosis. Notably, the platform can be used to detect *V. parahaemolyticus* and other pathogens or viruses via targeting of different crRNAs.

Supplementary Material

Supplementary material is available at *Food Quality and Safety* online.

Author Contributions

Jinbin Wang and Danhong Xu designed the study. Danhong Xu, Hua Liu, and Haijuan Zeng designed and performed the experiments and analyzed the data. Jinbin Wang, Danhong Xu, and Haijuan Zeng wrote and revised the manuscript. All the authors have read and approved the final version of this manuscript.

Funding

This study was supported by the Scientific and Innovative Action Plan of Shanghai (No.21N31900800), the Shanghai Rising-Star Program (No.23QB1403500), the Shanghai Science and Technology Commission, the Belt and Road Project (No.20310750500), the Talent Project of SAAS (No.2023–2025), and the SAAS Program for Excellent Research Team (No.2022 (B-16)), China.

Conflict of Interest

The authors declared that they have no conflicts of interest to this work. All authors have read and agreed to submit the manuscript.

References

Ashrafudoulla, M., Mizan, M. F. R., Park, S. H., *et al*. (2021). Current and future perspectives for controlling *Vibrio* biofilms in the seafood industry: a comprehensive review. *Critical Reviews in Food Science and Nutrition*, 61(11): 1827–1851.

Bai, N., Deng, W., Qi, Z., *et al*. (2023). The effect of alginate oligosaccharides on intestine barrier function and *Vibrio parahaemolyticus* infections in the white shrimp *Litopenaeus vannamei*. *Fish & Shellfish Immunology*, 141: 109011.

Boraschi-Diaz, I., Mort, J. S., Brömme, D., *et al*. (2018). Collagen type I degradation fragments act through the collagen receptor LAIR-1 to provide a negative feedback for osteoclast formation. *Bone*, 117: 23–30.

Campàs, M., Leonardo, S., Ferré-Gode, A., *et al*. (2023). Duplex electrochemical biosensor for the detection of the *tdh* and *trh* virulence genes of *Vibrio parahaemolyticus* in oysters. *Food Control*, 149: 109689.

Chaijarasphong, T., Thammachai, T., Itsathitphaisarn, O., *et al*. (2019). Potential application of CRISPR-Cas12a fluorescence assay coupled with rapid nucleic acid amplification for detection of white spot syndrome virus in shrimp. *Aquaculture*, 512: 734340.

Chamchoy, T., Okello, E., Williams, D. R., *et al*. (2022). Bayesian estimation of sensitivity and specificity of a rapid mastitis test kit, bacterial culture, and PCR for detection of *Staphylococcus aureus*, *Streptococcus* species, and coliforms in bovine milk samples. *Journal of Dairy Science*, 105(7): 6240–6250.

Chen, J. S., Ma, E. B., Harrington, L. B., *et al*. (2018). CRISPR-Cas12a target binding unleashes indiscriminate single-stranded DNase activity. *Science*, 360(6387): 791–791.

Chen, Y., Yang, T., Qian, S., *et al*. (2022). Multiple crRNAs-assisted CRISPR/Cas12a assay targeting cytochrome b gene for amplification-free detection of meat adulteration. *Analytica Chimica Acta*, 1231: 340417.

Collins, J. P., Shah, H. J., Weller, D. L., *et al*. (2022). Preliminary incidence and trends of infections caused by pathogens transmitted commonly through food—Foodborne Diseases Active Surveillance Network, 10 U.S. sites, 2016–2021. *Morbidity and Mortality Weekly Report*, 71(40): 1260–1264.

Fernandez, J. P., Vejnar, C. E., Giraldez, A. J., *et al*. (2018). Optimized CRISPR-Cpf1 system for genome editing in zebrafish. *Methods*, 150: 11–18.

Hille, F., Richter, H., Wong, S. P., *et al*. (2018). The biology of CRISPR-Cas: backward and forward. *Cell*, 172(6): 1239–1259.

Hu, Y. Q., Wang, W. Y., Fath, T., *et al*. (2023). Rapid and simultaneous detection of viable *Vibrio parahaemolyticus*, *Vibrio alginolyticus*, and *Vibrio cholerae* by PMA-mPCR assay in aquatic products. *LWT-Food Science and Technology*, 180: 114663.

Hyun, D. Y. (2009). Chapter 128: *Vibrio parahaemolyticus*. In: Feigin, R. D., Cherry, J. D., Demmler-Harrison, G. J., *et al*. S(Eds.). Feigin and Cherry's Textbook of Pediatric Infectious Diseases, 6th Edition. W.B. Saunders, Philadelphia, PA, USA, pp. 1625–1629.

Kilic, A., Basustaoglu, A. C. (2011). Double triplex real-time PCR assay for simultaneous detection of *Staphylococcus aureus*, *Staphylococcus epidermidis*, *Staphylococcus hominis*, and *Staphylococcus haemolyticus* and determination of their methicillin resistance directly from positive blood culture bottles. *Research in Microbiology*, 162(10): 1060–1066.

Li, S. Y., Cheng, Q. X., Liu, J. K., *et al*. (2018). CRISPR-Cas12a has both *cis*- and *trans*-cleavage activities on single-stranded DNA. *Cell Research*, 28(4): 491–493.

Lin, L., Zha, G., Wei, H., *et al*. (2023). Rapid detection of *Staphylococcus aureus* in food safety using an RPA-CRISPR-Cas12a assay. *Food Control*, 145: 109505.

Liu, H., Wang, J., Hu, X., *et al*. (2023). A rapid and high-throughput *Helicobacter pylori* RPA-CRISPR/Cas12a-based nucleic acid detection system. *Clinica Chimica Acta*, 540: 117201.

Makarova, K. S., Wolf, Y. I., Alkhnbashi, O. S., *et al*. (2015). An updated evolutionary classification of CRISPR–Cas systems. *Nature Reviews Microbiology*, 13(11): 722–736.

Neil, W. A., Hard, C., Bowers, J. C., *et al*. (2023). Levels of *Vibrio parahaemolyticus* in Pacific Oysters (*Crassostrea gigas*) from Washington State following ambient exposure and chilling. *Journal of Food Protection*, 86(6): 100092.

Nguyen, T. T. Q., Gu, M. B. (2023). An ultrasensitive electrochemical aptasensor using Tyramide-assisted enzyme multiplication for the detection of *Staphylococcus aureus*. *Biosensors and Bioelectronics*, 228: 115199.

NHC, SAMR (National Health Commission of the People's Republic of China, State Administration for Market Regulation). (2016). National Food Safety Standard Food Microbiological Examination: *Staphylococcus aureus*, GB 4789.10-2016. China Standards Press, Beijing, China. (in Chinese)

NHC, SAMR. (2021). National Standard for Food Safety, the Limit of Pathogenic Bacteria in Pre-Packaged Food, GB 29921-2021. China Standards Press, Beijing, China. (in Chinese)

Rosilan, N. F., Waiho, K., Fazhan, H., *et al*. (2023). Protein–protein interaction network analysis on the whiteleg shrimp *Penaeus vannamei* and *Vibrio parahaemolyticus* host–pathogen relationship reveals possible proteins and pathways involved during infection. *Aquaculture Reports*, 30: 101583.

Su, A., Liu, Y., Cao, X., *et al*. (2022). A universal CRISPR/Cas12a-mediated AuNPs aggregation-based surface-enhanced Raman scattering (CRISPR/Cas-SERS) platform for virus gene detection. *Sensors and Actuators B: Chemical*, 369: 132295.

Wang, W., Xiao, S., Zeng, M., *et al*. (2023). Dual-mode colorimetric-electrochemical biosensor for *Vibrio parahaemolyticus* detection based on CuO_2 nanodot-encapsulated metal–organic framework nanozymes. *Sensors and Actuators B: Chemical*, 387: 133835.

Wei, W., Haruna, S. A., Zhao, Y., *et al*. (2022). Surface-enhanced Raman scattering biosensor-based sandwich-type for facile and sensitive detection of *Staphylococcus aureus*. *Sensors and Actuators B: Chemical*, 364: 131929.

Xiao, Y., Ren, H., Wang, H., *et al*. (2023). A rapid and inexpensive nucleic acid detection platform for *Listeria monocytogenes* based on the CRISPR/Cas12a system. *Talanta*, 259: 124558.

Yin, C., Pang, B., Huang, Y., *et al*. (2023). Multiplex polymerase spiral reaction for simultaneous detection of *Salmonella typhimurium* and *Staphylococcus aureus*. *Analytical Biochemistry*, 667: 115086.

Yu, H., Rhee, M. S. (2023). Characterization of ready-to-eat fish surface as a potential source of contamination of *Vibrio parahaemolyticus* biofilms. *Food Research International*, 169: 112890.

Zha, S., Zhang, W., Liu, H., *et al*. (2023). Two common nanoparticles exert immunostimulatory and protective effects in *Tegillarca granosa* against *Vibrio parahaemolyticus*. *Fish & Shellfish Immunology*, 137: 108774.

Zhou, W., Wen, H., Hao, G., *et al*. (2023). Surface engineering of magnetic peroxidase mimic using bacteriophage for high-sensitivity/specificity colorimetric determination of *Staphylococcus aureus* in food. *Food Chemistry*, 426: 136611.